

New constraint on Europa's ice shell: Magnetic signature from the ocean

F. Daniel

Joint work with: C. Gissinger, L. Petitdemange

SF2A, Grenoble, 24 juin 2026



Northwestern
University

Contents

- 1 Magnetically-driven subsurface ocean of Europa
 - Numerical model
 - Results: global aspect
 - Results: local aspect

Outline

- 1 Magnetically-driven subsurface ocean of Europa
 - Numerical model
 - Results: global aspect
 - Results: local aspect

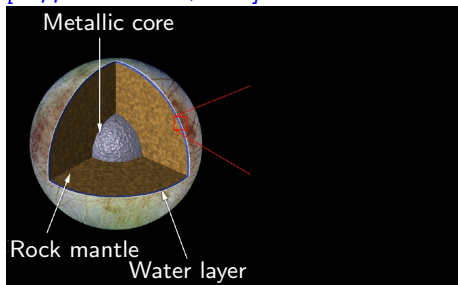
Europa



© Galileo space mission

Europa: some figures

[Pappalardo et al., 1999]

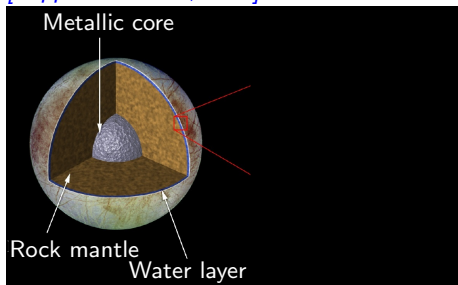


[Vance et al. 2018, Soderlund et al. 2020]

- Radius ~ 1560 km

Europa: some figures

[Pappalardo et al., 1999]

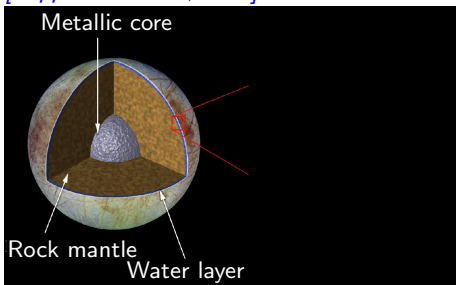


[Vance et al. 2018, Soderlund et al. 2020]

- Radius $\sim 1560 \text{ km}$
 - Metallic core $\sim 500 \text{ km}$

Europa: some figures

[Pappalardo et al., 1999]

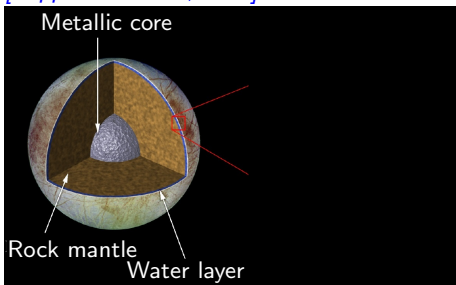


[Vance et al. 2018, Soderlund et al. 2020]

- Radius $\sim 1560 \text{ km}$
 - Metallic core $\sim 500 \text{ km}$
 - Rock mantle $\sim 1000 \text{ km}$

Europa: some figures

[Pappalardo et al., 1999]

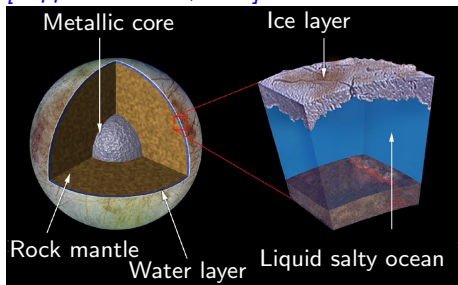


[Vance et al. 2018, Soderlund et al. 2020]

- Radius $\sim 1560 \text{ km}$
 - Metallic core $\sim 500 \text{ km}$
 - Rock mantle $\sim 1000 \text{ km}$
 - Water layer $\sim 100 \text{ km}$

Europa: some figures

[Pappalardo et al., 1999]

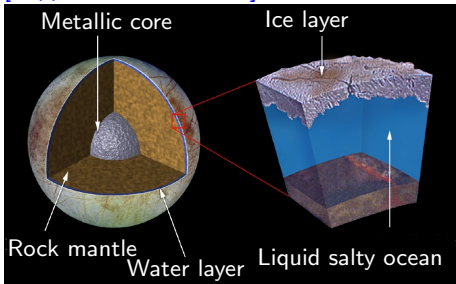


[Vance et al. 2018, Soderlund et al. 2020]

- Radius $\sim 1560 \text{ km}$
 - Metallic core $\sim 500 \text{ km}$
 - Rock mantle $\sim 1000 \text{ km}$
 - Water layer $\sim 100 \text{ km}$
- Ice $\sim 5 - 30 \text{ km}$
- **Liquid ocean** $\sim 80 - 130 \text{ km}$

Europa: Fluid Dynamics

[Pappalardo et al., 1999]

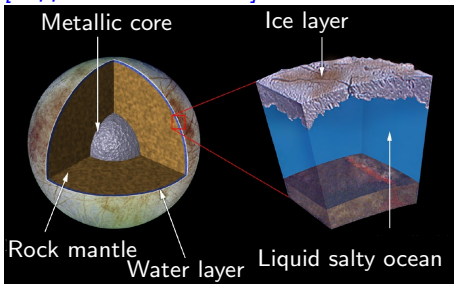


[Vance et al. 2018]

- Radius $\sim 1560km$
- Ice $\in [5 - 30]km$
- Salty ocean $\in [80 - 130]km$

Europa: Fluid Dynamics

[Pappalardo et al., 1999]



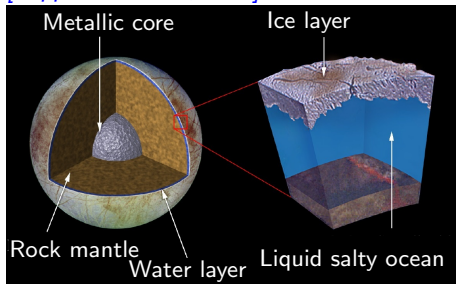
[Vance et al. 2018]

- Radius $\sim 1560km$
- Ice $\in [5 - 30]km$
- Salty ocean $\in [80 - 130]km$

Model Europa's subsurface ocean to predict the thickness of the ice

Europa: Fluid Dynamics

[Pappalardo et al., 1999]



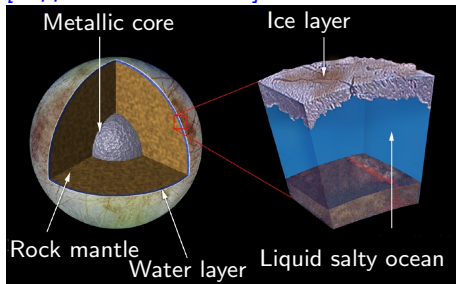
Possible forcing

- Convection [Soderlund et al., 2014, Gastine et al., 2016]
- Tides [Tyler 2008, Lemasquerier et al. 2023]
- Magnetic field of Jupiter [Gissinger and Petitdemange 2019, Daniel et al. 2025]
- Inertial waves [Rovira-Navarro 2018]
- Libration [Rekier et al. 2019]
- Double-diffusion [Wong et al. 2022]
- Melting [Gastine and Favier 2025]
- ...

Model Europa's subsurface ocean to predict the thickness of the ice

Europa: Fluid Dynamics

[Pappalardo et al., 1999]



Possible forcing

- Convection [Soderlund et al., 2014, Gastine et al., 2016]
- Tides [Tyler 2008, Lemasquerier et al. 2023]
- Magnetic field of Jupiter [Gissinger and Petitdemange 2019, Daniel et al. 2025]
- Inertial waves [Rovira-Navarro 2018]
- Libration [Rekier et al. 2019]
- Double-diffusion [Wong et al. 2022]
- Melting [Gastine and Favier 2025]
- ...

Model Europa's subsurface ocean to predict the thickness of the ice

Europa: Fluid Dynamics

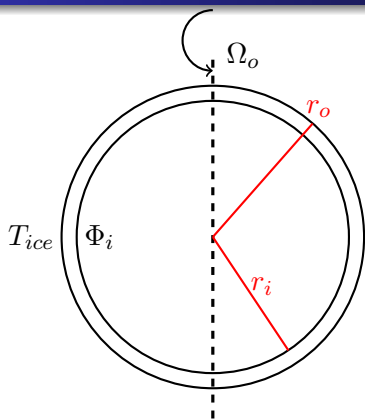


Possible forcing

- Convection [*Soderlund et al., 2014, Gastine et al., 2016*]
- Tides [*Tyler 2008, Lemasquerier et al. 2023*]
- Magnetic field of Jupiter [*Gissinger and Petitdemange 2019, Daniel et al. 2025*]
- Inertial waves [*Rovira-Navarro 2018*]
- Libration [*Rekier et al. 2019*]
- Double-diffusion [*Wong et al. 2022*]
- Melting [*Gastine and Favier 2025*]
- ...

Model Europa's subsurface ocean to predict the thickness of the ice

Simulations



- Solve for $\mathbf{u}, \mathbf{B}, T$
- $r_i/r_o = 0.9$ (Europa 0.92 – 0.94)
- Boussinesq
- constant ν, κ, η
- $d = r_o - r_i$

- BC for u : no slip
- BC for B : insulating
- BC for T : imposed flux at r_i and temperature at r_o
- Oscillating magnetic field $B_0(t)$
- PaRoDy code [*Dormy 1998, Aubert 2008, Schaeffer 2013*]

Dimensionless parameters

$$Ra^Q = \frac{\alpha_T \Phi_i g_o r_o^2 r_i^2}{\nu \kappa k}, \quad Ek = \frac{\nu}{r_o^2 \Omega_o}, \quad \tilde{\Lambda} = \frac{B_o^2}{\rho \mu_0 \nu \Omega_o}, \quad Pr = \frac{\nu}{\kappa}, \quad Ek_\eta = \frac{\eta}{r_o^2 \Omega_o}$$

	Ra^Q	Ek	$\tilde{\Lambda}$	Pr	Ek_η
DNS	$10^5 - 10^{12}$	$10^{-5} - 10^{-4}$	$1 - 3 \cdot 10^3$	12	10^{-2}
Europa	$10^{31} - 10^{32}$	$10^{-14} - 10^{-13}$	10	12	$10^{-3} - 10^{-2}$

Dimensionless parameters

$$Ra^Q = \frac{\alpha_T \Phi_i g_o r_o^2 r_i^2}{\nu \kappa k}, \quad Ek = \frac{\nu}{r_o^2 \Omega_o}, \quad \tilde{\Lambda} = \frac{B_o^2}{\rho \mu_0 \nu \Omega_o}, \quad Pr = \frac{\nu}{\kappa}, \quad Ek_\eta = \frac{\eta}{r_o^2 \Omega_o}$$

	Ra^Q	Ek	$\tilde{\Lambda}$	Pr	Ek_η
DNS	$10^5 - 10^{12}$	$10^{-5} - 10^{-4}$	$1 - 3 \cdot 10^3$	12	10^{-2}
Europa	$10^{31} - 10^{32}$	$10^{-14} - 10^{-13}$	10	12	$10^{-3} - 10^{-2}$

Two forcing terms

- thermal Ra^Q
- magnetic $\tilde{\Lambda}$

Dimensionless parameters

$$Ra^Q = \frac{\alpha_T \Phi_i g_o r_o^2 r_i^2}{\nu \kappa k}, \quad Ek = \frac{\nu}{r_o^2 \Omega_o}, \quad \tilde{\Lambda} = \frac{B_o^2}{\rho \mu_o \nu \Omega_o}, \quad Pr = \frac{\nu}{\kappa}, \quad Ek_\eta = \frac{\eta}{r_o^2 \Omega_o}$$

	Ra^Q	Ek	$\tilde{\Lambda}$	Pr	Ek_η
DNS	$10^5 - 10^{12}$	$10^{-5} - 10^{-4}$	$1 - 3 \cdot 10^3$	12	10^{-2}
Europa	$10^{31} - 10^{32}$	$10^{-14} - 10^{-13}$	10	12	$10^{-3} - 10^{-2}$

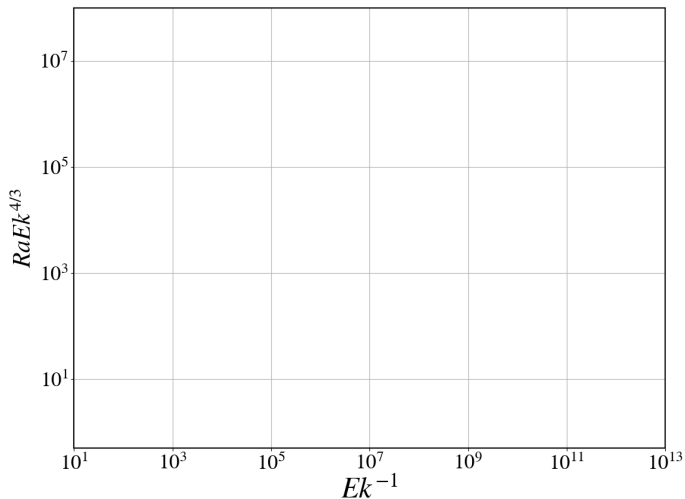
Two forcing terms

- thermal Ra^Q
- magnetic $\tilde{\Lambda}$

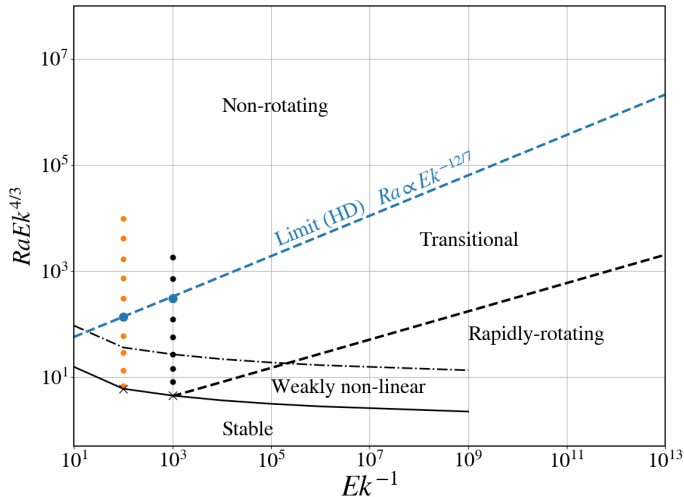
Outputs:

- e.g. $Nu = \frac{\Phi}{k \Delta T / d}$

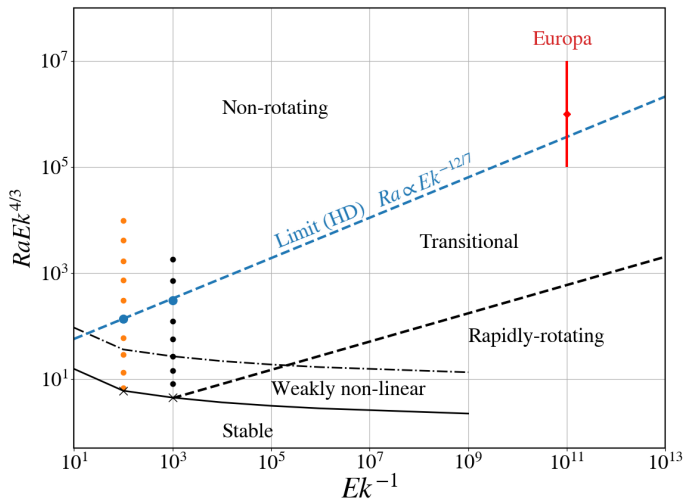
Limit $\Lambda = 0$: Rotating Rayleigh-Bénard convection



Limit $\Lambda = 0$: Rotating Rayleigh-Bénard convection



Limit $\Lambda = 0$: Rotating Rayleigh-Bénard convection



Limit $\Lambda = 0$: Rotating Rayleigh-Bénard convection

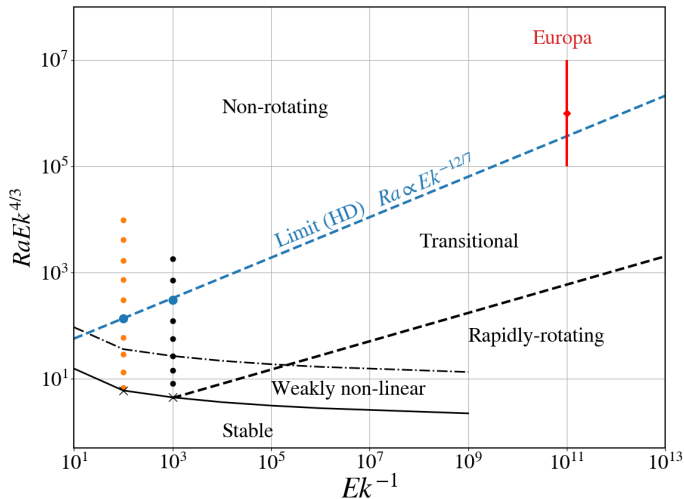


Figure: Regime diagram adapted from [Lemasquerier et al., 2023] and [Gastine et al., 2016] for RRBC.

Limit $\Lambda = 0$: Rotating Rayleigh-Bénard convection

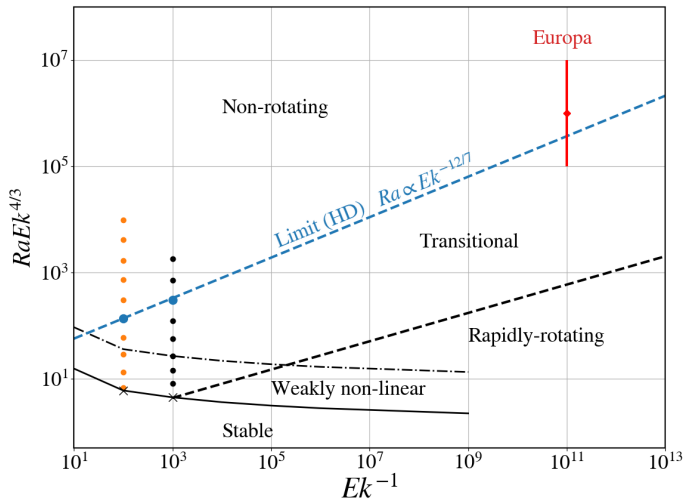
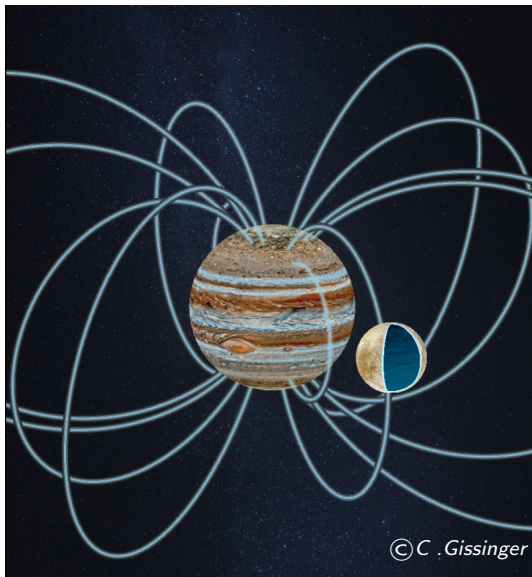


Figure: Regime diagram adapted from [Lemasquerier et al., 2023] and [Gastine et al., 2016] for RRBC. Purely hydrodynamical

Limit $Ra^Q = 0$



$$\text{Limit } Ra^Q = 0$$

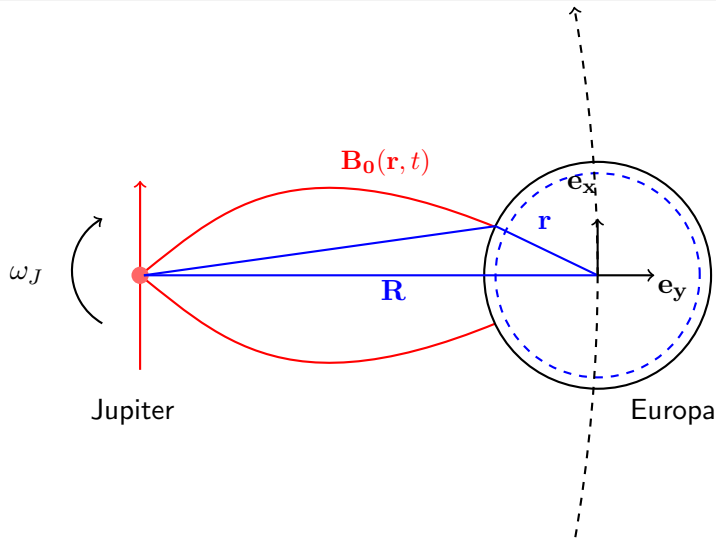


Figure: Top view sketch

Limit $Ra^Q = 0$: Geometry and amplitude of the flow

[Gissinger and Petitdemange 2019]

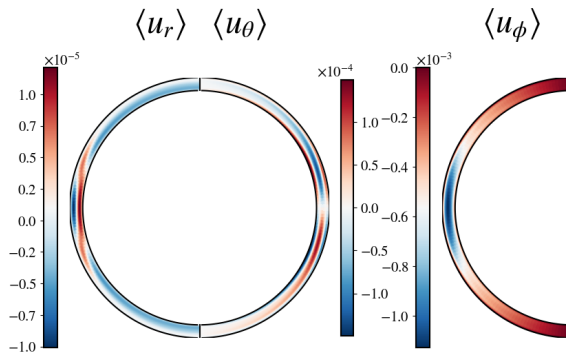
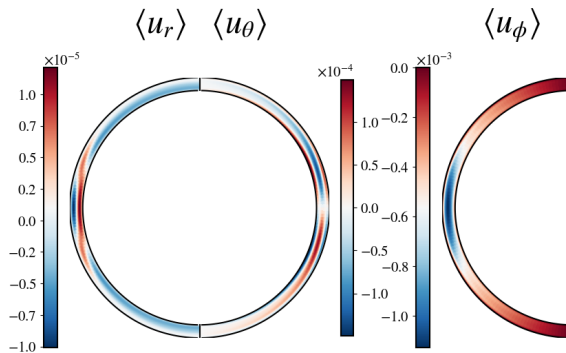


Figure: Meridional cuts of azimuthally averaged u_r , u_θ , u_ϕ for $Ek = 10^{-4}$, $\tilde{\Lambda} = 1$.

Limit $Ra^Q = 0$: Geometry and amplitude of the flow [Gissinger and Petitdemange 2019]



Estimate of the jet
velocity for Europa:

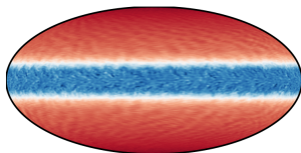
1 – 100 cm/s

Figure: Meridional cuts of azimuthally averaged u_r , u_θ , u_ϕ for $Ek = 10^{-4}$, $\tilde{\Lambda} = 1$.

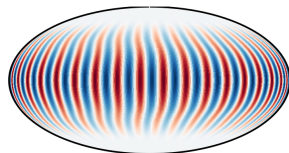
Combined forcings: $\Lambda, Ra^Q \neq 0$

- Fixed rotation $Ek = 10^{-4}$
- Four different amplitudes of the jet $\tilde{\Lambda} \in [1, 10, 100, 3000]$
- Increase Ra^Q
- Known threshold of convection for $\tilde{\Lambda} = 0$

$$Nu = \frac{\Phi}{k\Delta T/d} \quad (1)$$



Magnetically-driven jet



Convection

Combined forcings: $\Lambda, Ra^Q \neq 0$

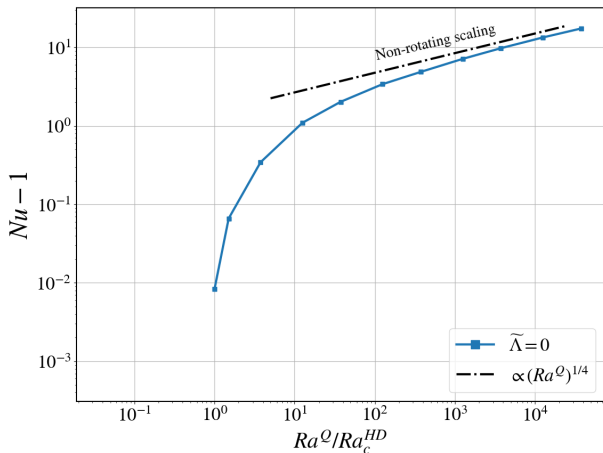


Figure: Evolution of the Nusselt number for $Ek = 10^{-4}$, $Ek_\eta = 10^{-2}$, $Pr = 12$ and different values of $\tilde{\Lambda}$.

Combined forcings: $\Lambda, Ra^Q \neq 0$

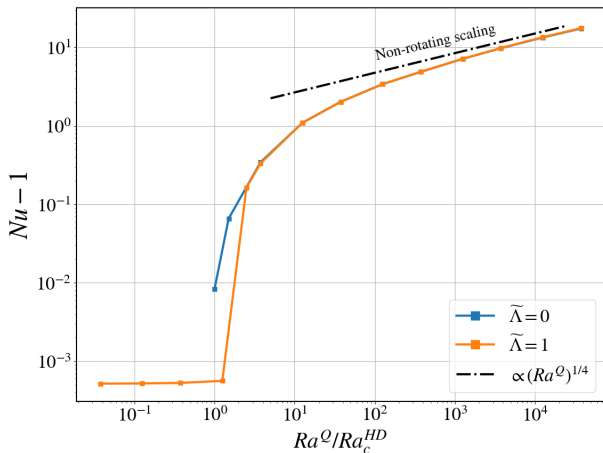


Figure: Evolution of the Nusselt number for $Ek = 10^{-4}$, $Ek_\eta = 10^{-2}$, $Pr = 12$ and different values of $\tilde{\Lambda}$.

Combined forcings: $\Lambda, Ra^Q \neq 0$

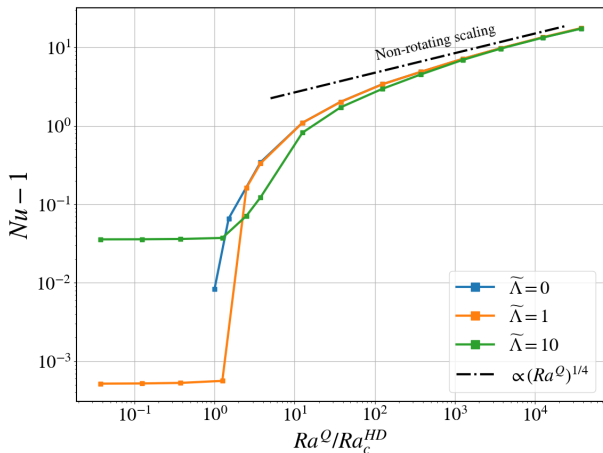


Figure: Evolution of the Nusselt number for $Ek = 10^{-4}$, $Ek_\eta = 10^{-2}$, $Pr = 12$ and different values of $\tilde{\Lambda}$.

Combined forcings: $\Lambda, Ra^Q \neq 0$

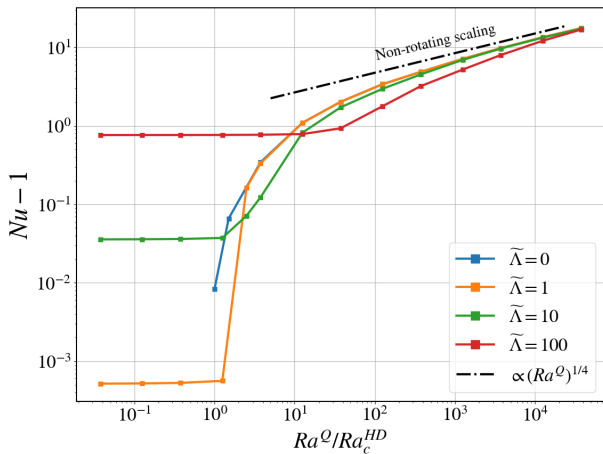


Figure: Evolution of the Nusselt number for $Ek = 10^{-4}$, $Ek_\eta = 10^{-2}$, $Pr = 12$ and different values of $\tilde{\Lambda}$.

Combined forcings: $\Lambda, Ra^Q \neq 0$

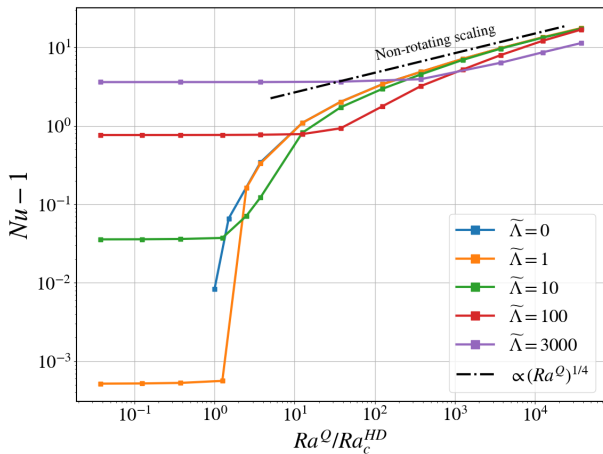


Figure: Evolution of the Nusselt number for $Ek = 10^{-4}$, $Ek_\eta = 10^{-2}$, $Pr = 12$ and different values of $\tilde{\Lambda}$.

Modified thresholds: transition to NR regime

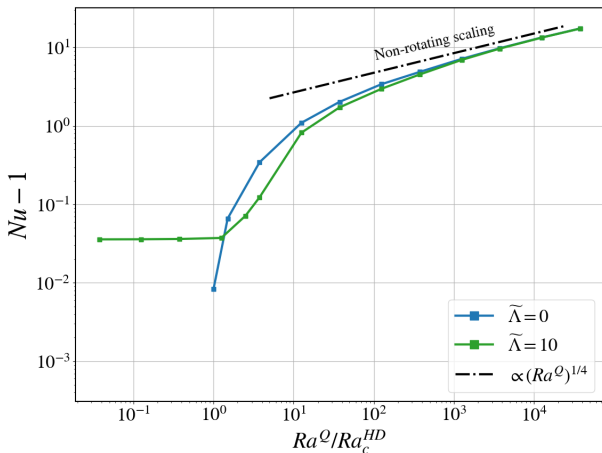


Figure: Evolution of the Nusselt number for $Ek = 10^{-4}$, $Ek_\eta = 10^{-2}$, $Pr = 12$ and different values of $\tilde{\Lambda}$.

Modified thresholds: transition to NR regime

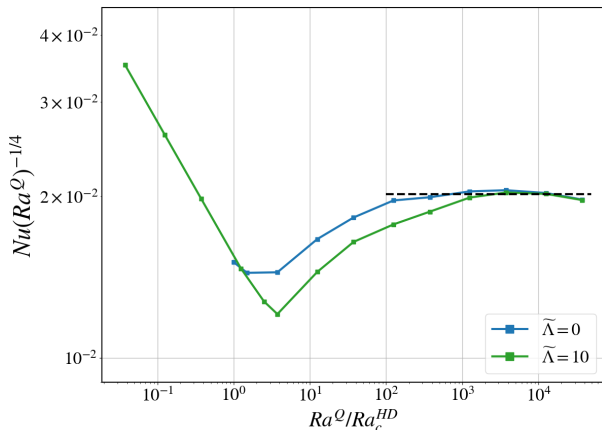


Figure: Evolution of $Nu(Ra^Q)^{-1/4}$ for $\tilde{\Lambda} = 0$ or 10 for $Ek = 10^{-4}$, $Ek_\eta = 10^{-2}$, $Pr = 12$.

Modified thresholds: transition to NR regime

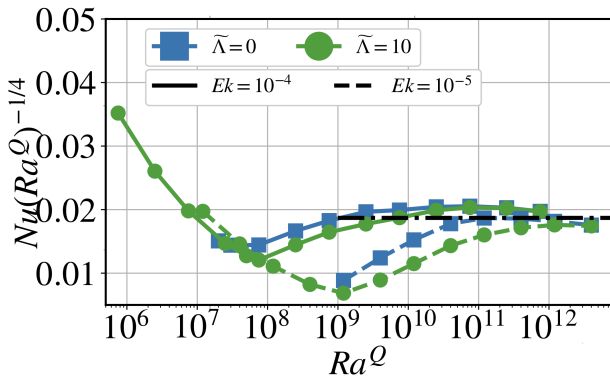
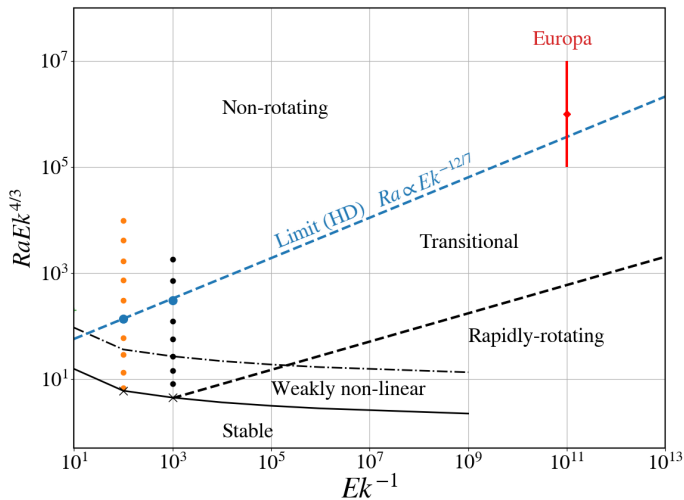
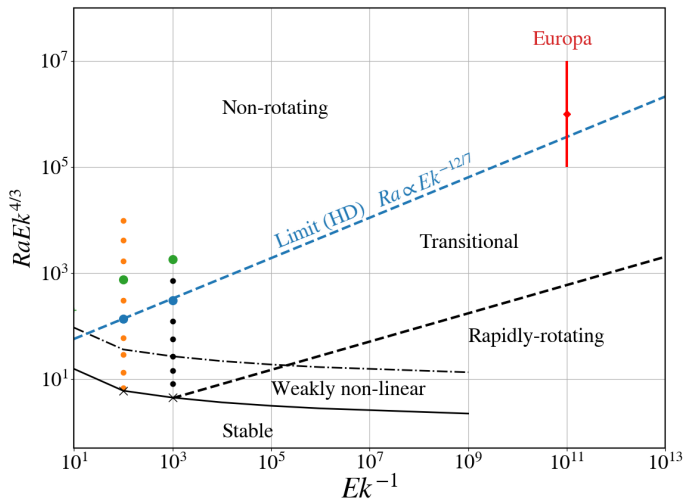


Figure: Evolution of $Nu(Ra^Q)^{-1/4}$ for $\tilde{\Lambda} = 0$ or 10 for $Ek = 10^{-4}$, $Ek_\eta = 10^{-2}$, $Pr = 12$.

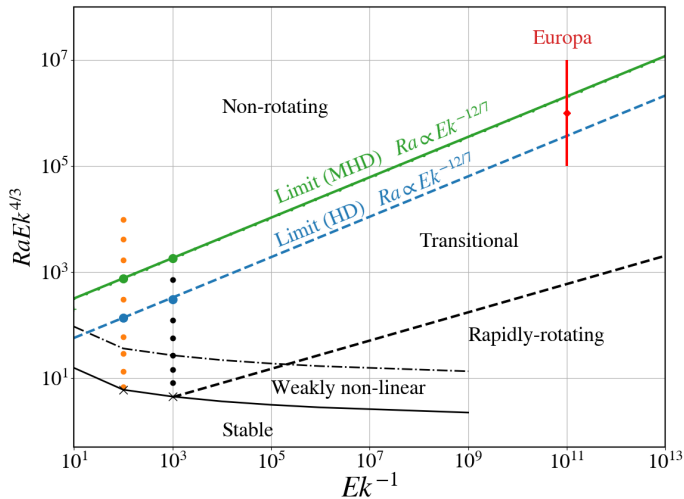
What about Europa? Importance of the thresholds



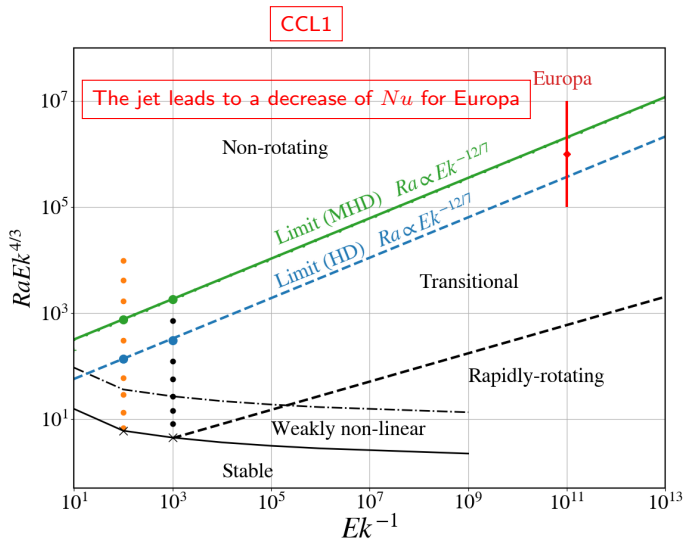
What about Europa? Importance of the thresholds



What about Europa? Importance of the thresholds



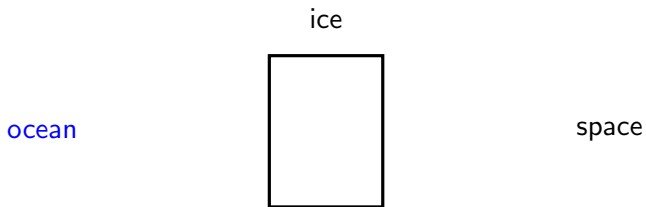
What about Europa? Importance of the thresholds



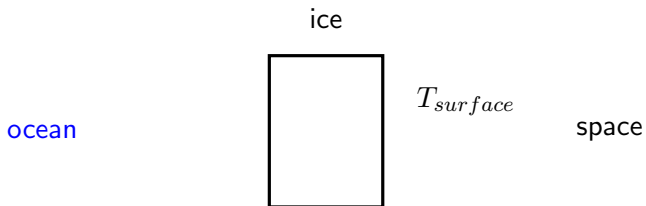
[Daniel et al.2025]

Heat flux and ice thickness

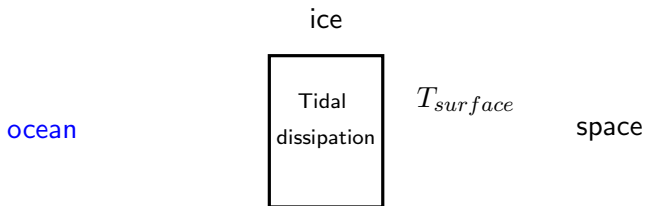
Heat flux and ice thickness



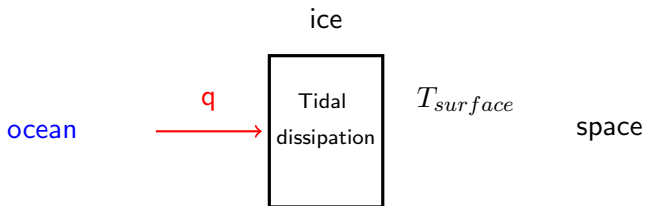
Heat flux and ice thickness



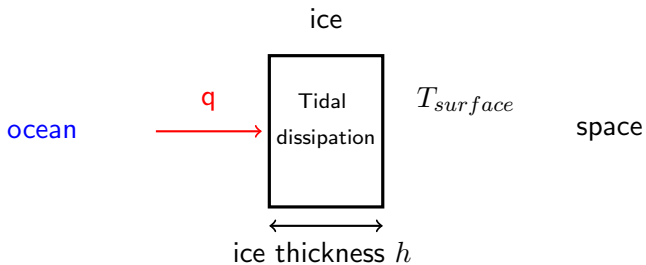
Heat flux and ice thickness



Heat flux and ice thickness

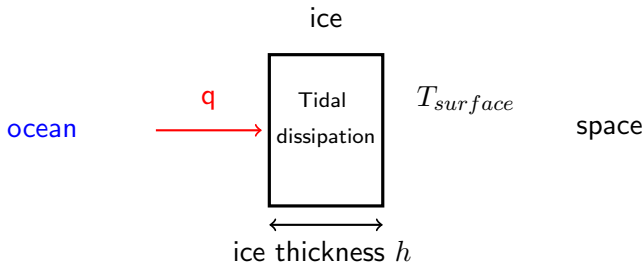


Heat flux and ice thickness



Heat flux and ice thickness

Heat flux at the ice/ocean interface $q = -k \frac{\partial T}{\partial r} |_{r=r_o}$: constraint on the ice thickness h [Nimmo et al. 2007].



Heat flux and ice thickness (HD)

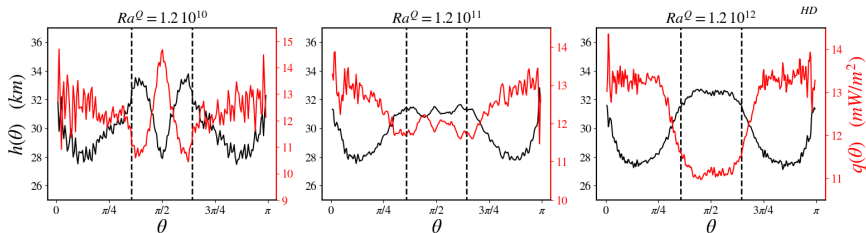


Figure: Evolution of q and h with Ra^Q for $Ek = 10^{-5}$, $Ek_\eta = 10^{-2}$, $Pr = 12$, $\tilde{\Lambda} = 0$.

Heat flux and ice thickness (MHD)

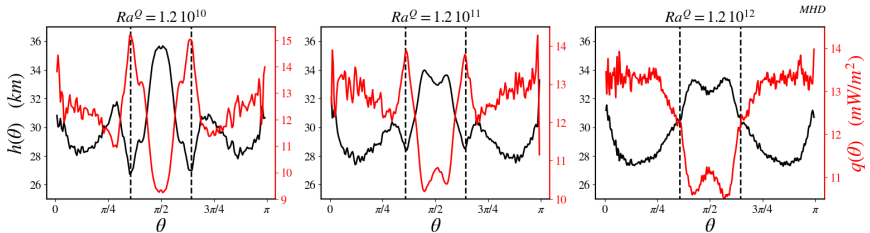


Figure: Evolution of q and h with Ra^Q for $Ek = 10^{-5}$, $Ek_\eta = 10^{-2}$, $Pr = 12$, $\tilde{\Lambda} = 10$.

Ice thickness (MHD vs HD)

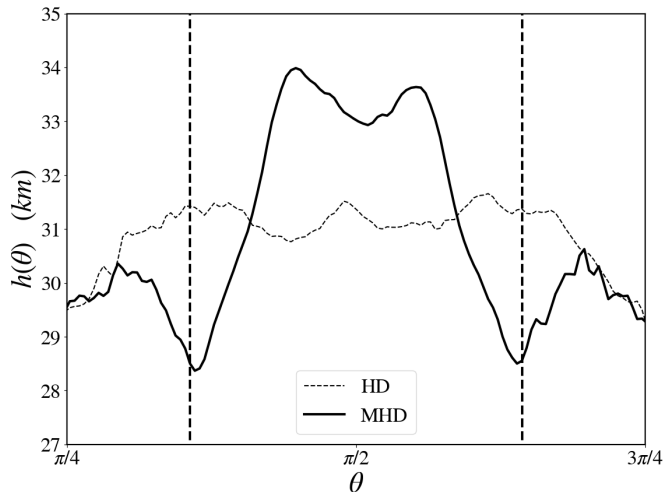


Figure: Magnified comparison for h with $Ra^Q = 1.2 \cdot 10^{11}$ for $Ek = 10^{-5}$, $Ek_\eta = 10^{-2}$, $Pr = 12$, $\tilde{\Lambda} = 10$. [Daniel et al.2025]

Ice thickness (MHD vs HD)

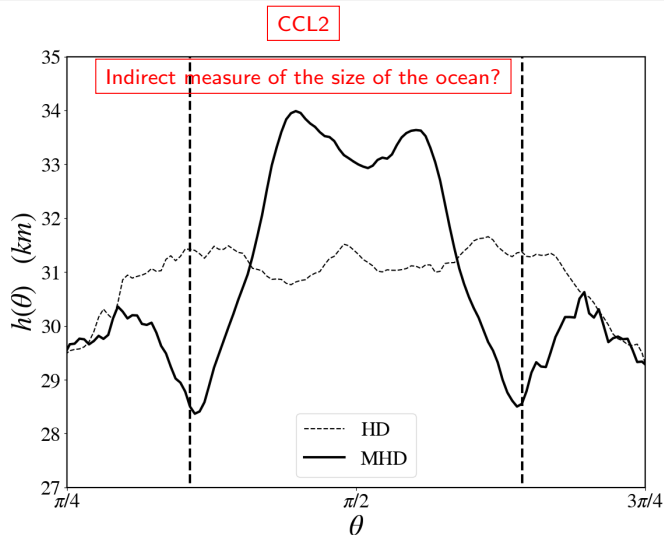


Figure: Magnified comparison for h with $Ra^Q = 1.2 \cdot 10^{11}$ for $Ek = 10^{-5}$, $Ek_\eta = 10^{-2}$, $Pr = 12$, $\tilde{\Lambda} = 10$. [Daniel et al.2025]

General conclusion

Numerical model of Europa's ocean

- Modification of rotating convection properties → Magnetically-driven jet
- Local impact for the ice thickness due to the presence of the jet

General conclusion

Numerical model of Europa's ocean

- Modification of rotating convection properties → Magnetically-driven jet
- Local impact for the ice thickness due to the presence of the jet

Perspectives

General conclusion

Numerical model of Europa's ocean

- Modification of rotating convection properties → Magnetically-driven jet
- Local impact for the ice thickness due to the presence of the jet

Perspectives

- DNS: Other physical phenomena: melting, tidal forcing

General conclusion

Numerical model of Europa's ocean

- Modification of rotating convection properties → Magnetically-driven jet
- Local impact for the ice thickness due to the presence of the jet

Perspectives

- DNS: Other physical phenomena: melting, tidal forcing
- Space missions: measurements

General conclusion

Numerical model of Europa's ocean

- Modification of rotating convection properties → Magnetically-driven jet
- Local impact for the ice thickness due to the presence of the jet

Perspectives

- DNS: Other physical phenomena: melting, tidal forcing
- Space missions: measurements

Daniel, F., Petitdemange, L. and Gissinger, C. (2025). *New constraint on Europa's ice shell: Magnetic signature from the ocean*. Icarus, 116792.

Appendix: MHD equations for an incompressible flow using Boussinesq approximation

$$\frac{\partial \mathbf{u}}{\partial t} + \mathbf{u} \cdot \nabla \mathbf{u} + 2\boldsymbol{\Omega}_o \times \mathbf{u} = -\nabla \Pi / \rho + \nu \Delta \mathbf{u} + \alpha_T g(r) T \mathbf{e}_r + (\rho \mu_0)^{-1} (\nabla \times \mathbf{B}) \times \mathbf{B}, \quad (2)$$

$$\frac{\partial T}{\partial t} + \mathbf{u} \cdot \nabla T = \kappa \Delta T, \quad (3)$$

$$\frac{\partial \mathbf{B}}{\partial t} = \nabla \times (\mathbf{u} \times \mathbf{B}) + \eta \Delta \mathbf{B}, \quad (4)$$

$$\nabla \cdot \mathbf{u} = 0, \quad (5)$$

$$\nabla \cdot \mathbf{B} = 0, \quad (6)$$

Pseudo-spectral code PaRoDy [[Dormy 1998](#), [Aubert 2008](#)] with SHTns [[Schaeffer 2013](#)]

Appendix: Limit $Ra^Q = 0$: Amplitude of the recirculation

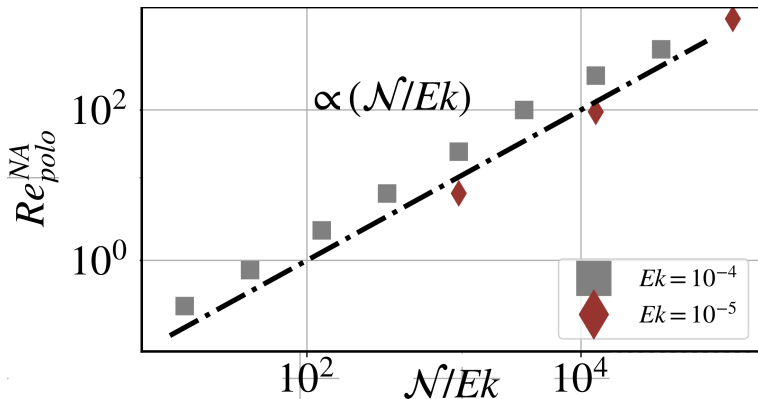


Figure: Amplitude of the velocity of the poloidal recirculation as a function of $\mathcal{N} = B_o^2 \eta / (\rho \mu_0 \nu c^2)$. [Daniel et al. 2025]

Appendix: Limit $Ra^Q = 0$: Heat transport due to the recirculation

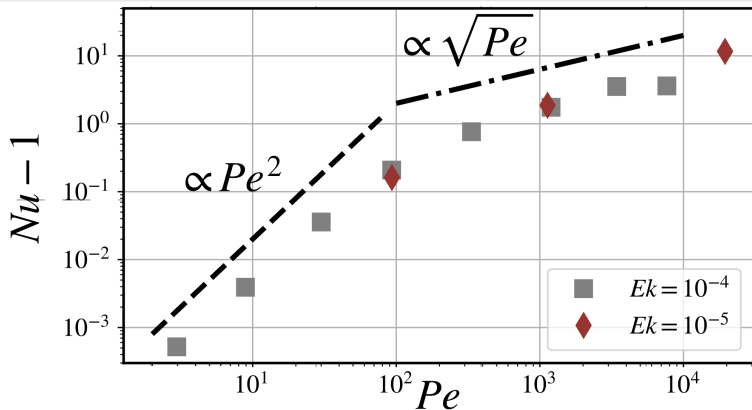


Figure: Evolution of the Nusselt number against the Péclet number $Pe = U_{jet} r_o / \kappa$ due to the Jovian field for two levels of rotation. [Daniel et al. 2025]

Appendix: Limit $Ra^Q = 0$: Heat transport due to the recirculation

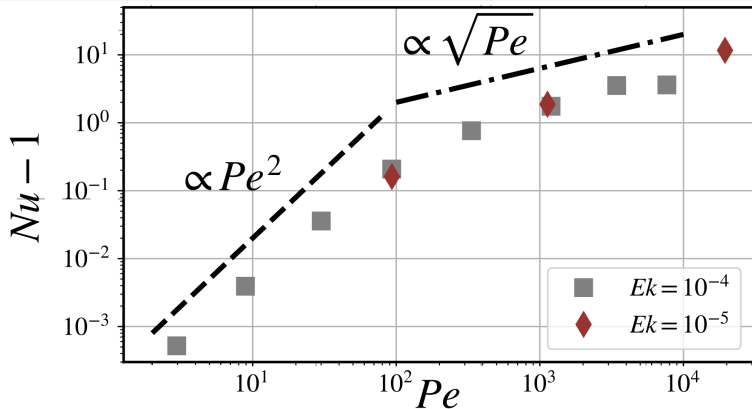


Figure: Evolution of the Nusselt number against the Péclet number $Pe = U_{jet} r_o / \kappa$ due to the Jovian field for two levels of rotation. [Daniel et al. 2025]

Appendix: Can it be observed?

~~ice thickness h~~ → topography of the satellite

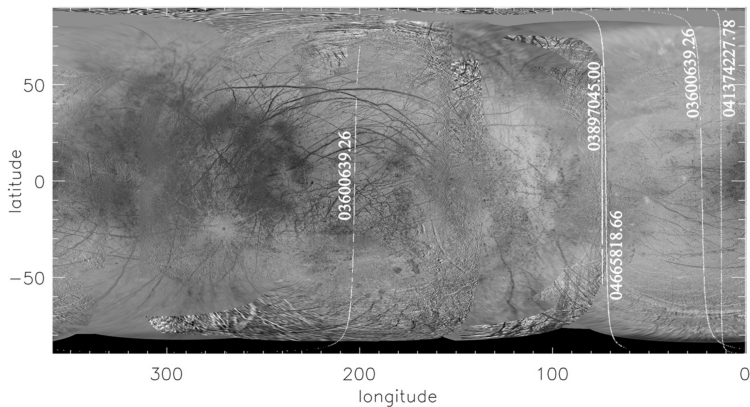


Figure: Limb profile measurements [Nimmo et al.2007]

Appendix: Comparisons with observations

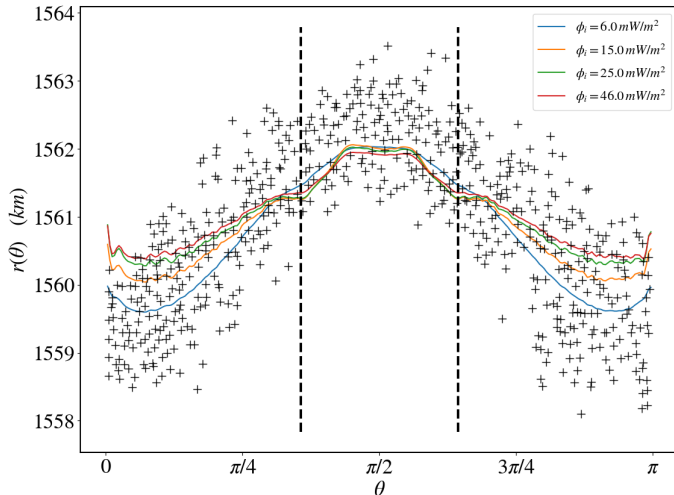


Figure: Radial profile of Europa, DNS vs observations ([Nimmo et al.2007]) for different ocean's floor heat flux values. [Daniel et al.2025]

Appendix: Comparisons with observations

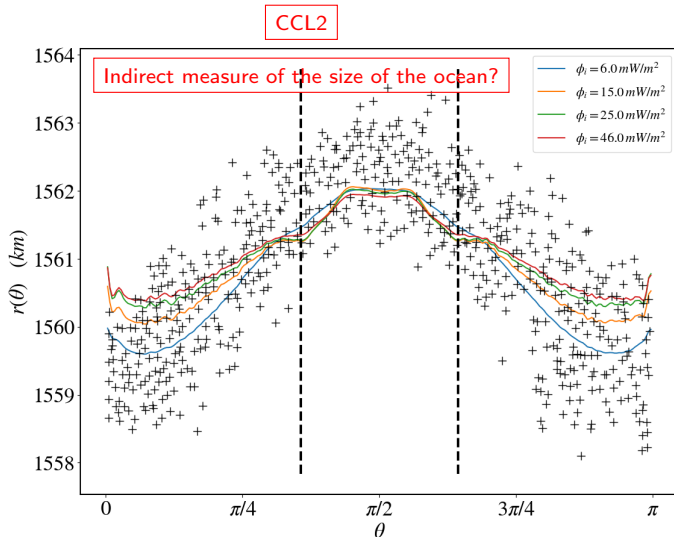


Figure: Radial profile of Europa, DNS vs observations ([Nimmo et al.2007]) for different ocean's floor heat flux values. [Daniel et al.2025]